A 14q distal chromoanagenesis elucidated by whole genome sequencing

Flavie Ader, Solveig Heide, Pauline Marzin, Alexandra Afenjar, Flavie Diguet, Sandra Chantot Bastaraud, Pierre-Antoine Rollat-Farnier, Damien Sanlaville, Marie-France Portnoï, Jean-Pierre Siffroi, et al.

A 14q Distal Chromoanagenesis elucidated by whole genome sequencing.

Flavie Ader [a*], Solveig Heide [a], Pauline Marzin[a], Alexandra Afenjar [b], Flavie Diguet [c,e], Sandra Chantot Bastaraud [a], Pierre-Antoine Rollat-Farnier [c,d], Damien Sanlaville [c,e], Marie-France Portnoï [a], Jean-Pierre Siffroi,[a], Caroline Schluth-Bolard [c,e]

[a] Sorbonne Université, Physiopathologie des Maladies Génétiques d'Expression Pédiatrique, F-75012 Paris, France.

[b] Unité de neuropédiatrie et pathologie du développement, GHU Paris Est - Hôpital d'Enfants Armand-Trousseau

[c] Service de Génétique, Laboratoire de Cytogénétique Constitutionnelle, Hospices Civils de Lyon, Bron, France

[d] Cellule bioinformatique de la plateforme NGS, Hospices Civils de Lyon, Bron, France

[e] GENDEV Team, Neurosciences Research Center of Lyon, INSERM U1028; CNRS UMR5292; UCBL1, 69677 BRON, France

*** Corresponding author**: flavie.ader@aphp.fr

ABSTRACT

Chromoanagenesis represents an extreme form of genomic rearrangements involving multiple breaks occurring on a single or multiple chromosomes. It has been recently described in both acquired and rare constitutional genetic disorders. Constitutional chromoanagenesis events could lead to abnormal phenotypes including developmental delay and congenital anomalies, and have also been implicated in some specific syndromic disorders. We report on a girl presenting with growth retardation, hypotonia, microcephaly, dysmorphic features, coloboma, and hypoplastic corpus callosum. Karyotype showed a *de novo* structurally abnormal chromosome 14q31qter region. Molecular characterization using SNP-array revealed a complex unbalanced rearrangement in 14q31.1-q32.2, on the paternal chromosome 14, including thirteen interstitial deletions ranging from 33kb to 1.56Mb in size, with a total of 4.1 Mb in size, thus suggesting that a single event like chromoanagenesis occurred. To our knowledge, this is one of the first case of 14q distal deletion due to a germline chromoanagenesis. Genome sequencing allowed the characterization of 50 breakpoints, leading to interruption of 10 genes including *YY1* which fit with the patient's phenotype. This precise genotyping of breaking junction allowed better definition of genotype-phenotype correlations.

KEY WORDS

chromoanagenesis; constitutionnal; intellectual disability; microcephaly; 14q deletion; coloboma; hypoplastic corpus callosum; genome sequencing

Introduction

Constitutional complex chromosome rearrangements (CCRs) are rare structural anomalies characterized by three or more breakpoints, involving at least a chromosome [1]. They are usually identified by standard karyotyping and further characterized by array-based analysis. Recently, highly complex changes termed chromoanagenesis, arising from shattering mechanisms, were observed in cancer genomes, and have also been described in rare patients with developmental disorders. Genomic imbalances included deletions, duplications and /or triplications, translocations and inversions, concentrated on a single or few chromosomes [2, 3, 4 ,5]. Depending of the mechanism of chromoanagenesis, several terms are used, chromotripsis referred to a mitotic event with chromosome shattering and non-homologous end joining repair; and chromoanasynthesis referred to a local defective DNA replication with microhomology-mediated template switching that produces local rearrangements with altered gene copy numbers. The presence of chromoanagenesis in healthy individuals affecting reproduction has also recently been reported [6, 7].

Here, we describe a complex 14q distal deletion consistent with a constitutional chromoanagenesis process, in a girl with developmental delay and congenital anomalies. Our patient shows clinical findings described in patients with 14q terminal deletion syndrome (developmental delay, hypotonia, growth retardation, microcephaly, a characteristic facial appearance and a variety of ocular anomalies, including retinal pigmentary changes, microphthalmia and coloboma) [8], especially ocular and brain malformations. The complexity of this case of chromoanagenesis, as well as the possibility to identify new genotype-phenotype relationships, has been elucidated by whole genome sequencing.

Clinical Report

The proband, an 8 month-old-girl, is the third child of healthy unrelated 42 years old mother and 38 years old father. The family history was negative for birth defects or developmental delay. The pregnancy had been complicated by maternal hypertension and intrauterine growth retardation (IUGR). Third trimester ultrasound examination revealed hypoplasia of the corpus callosum and reduction of the biparietal diameter. Cytogenetic analysis from amniotic cells performed in another institution showed an apparent normal 46,XX karyotype. She was born at 33+2 weeks of gestation after a caesarian section. Birth weight was 2050 g (< 3rd centile), birth length 43 cm (< 3rd centile) and head circumference 32 cm (3rd centile). After birth, she was hospitalized for one month because of hypotonia, feeding difficulties and growth retardation. Subsequently, hypertonic movements of the limbs were noted. At the age of 8 months, the neurological examination revealed axial hypotonia and peripheral hypertonia. She was unable to hold her head and to sit without support. She was not able to vocalize. She had a height of 60 cm (-3SD), a weight of 5100 g (-3SD), a microcephaly with a head circumference of 39 cm (-3SD) and a large anterior fontanel. Facial dysmorphic features included a broad and flat nasal bridge, epicanthus, a short nose, a broad philtrum, a small mouth with thin upper lip, and small and low-set ears. An electroencephalogram (EEG) gave normal results. Brain Magnetic resonance imaging (MRI) confirmed the corpus callosum hypoplasia. Ophthalmologic examination revealed bilateral chorioretinal coloboma. Echocardiography and renal ultrasound examination gave normal results. The patient died after a severe rhabdomyolysis event associated with multiorgan failure at the age of 2 years.

Investigations and Results

Cytogenetic analysis was performed again in our laboratory on GTG an RHG-banded metaphases from lymphocytes at a resolution of approximately 500 bands

according to the standard cytogenetic protocol (Fig. 1.A). FISH analyses using WCP 14 Probe (Metasystem, Altlussheim, Germany), tel 14q probe (Vysis, Illinois, Unated States) and bacterial artificial chromosome (BAC) probes targeting the rearranged 14q region, were realized according to standard procedures (Fig.1.B,C,D). Single nucleotide polymorphism (SNP) microarray analysis was performed using a Human OmniExpress24, which contains 713,599 markers including 395,094 SNPs (Illumina, San Diego, United States), according to the manufacturer's protocol. Results were analyzed with Illumina GenomeStudio software. SNP profiles were analyzed by comparing the Log R ratio, i.e., ln (sample copy number/ reference copy number), and the B allele frequency (BAF) (Fig 1.E,F). Data analysis was based on information from the UCSC Genome Browser (NCBI37 hg19).

G-banded chromosomes analysis revealed an abnormal female karyotype with structural changes spanning the terminal region of the long arm of one chromosome 14, in all the cells examined (Fig.1). Parental karyotypes were normal. Methylation specific PCR of the differentially methylated region at 14q32 showed normal biparental inheritance and no abnormality of methylation at the *GTL2/DKL1* region, confirming that the patient does not have chromosome 14 uniparental disomy (UPD). SNP array analysis revealed thirteen interstitial deletions of chromosome 14, between bands 14q31.1 and 14q32.2 (chr14: 83088298_100452660), ranged from 33 kb to 1.56 Mb in size, with a total of 4.1 Mb in size (Fig.1, supplemental data 1). These deletions were separated by normal copy number segments. The distal breakpoint was located at 740kb from the imprinted gene cluster. FISH analysis using BACs RP11-300J18 (14q31.3: 88484949_88502663) (Fig.1), RP11-543C4 (14q32.2: 100070893_100092077) confirmed the deletions. The BAC RP11-433J8 (14q32.2: 97059105_97061097) probe was not deleted. SNP-array analysis of deletions intervals

in the parents and patient revealed that the rearrangement derived from the paternal chromosome 14 (supplemental data 2).

For a better understanding of the mechanism of this event, whole genome sequencing (WGS) with break point analysis has been performed. A 350-bp fragments library was prepared following the Illumina TruSeq DNA PCR-free protocol (Illumina, San Diego, California, USA) with 3µg genomic DNA, according to manufacturer instructions. DNA library was sequenced on an Illumina NextSeq 500 as paired-end 101 bp reads using the High Output (300 cycles) NextSeq500 kit, yielding a mean sequencing depth of 14.32X. Image analysis and base calling were performed using Illumina Real Time Analysis Pipeline 2 with default parameters. Alignment of the reads against the hg19 version of the human genome was done using BWA-MEM v 0.7.10 [9]. The reads were sorted using Samtools v 1.3.1 [10], and the duplicates removed by PicardTools v 1.138 (picard.sourceforge.net). Structural variants (SV) were detected using BreakDancer v 1.4.5 [11] and annotated using an in-house program in order to filter out recurrent variants. Integrative Genomics Viewer v 2.3 [12] was used for the SV visualization and validation. Junction sequences were determined using split-read sequences when at least 2 split-reads were available. If not possible, junction fragments were amplified by PCR (junctions n°2, 6, 16, 20, 27, 28, 30, 41 and 46), in the patient and a control with no chromosomal rearrangement, using Taq DNA Core kit 10 (MP Biomedicals, Solon, Ohio), according manufacturer instructions followed by Sanger sequencing. Junctions sequences were then aligned using BLAT tool (UCSC) against hg19 reference in order to obtain the breakpoint at the base-pair level. WGS identified a highly complex rearrangement including 50 breakpoints on chromosome 14, clustered in the 14q31.1q32.33 region. In 8 breakpoints (n°2, 6, 16, 20, 27, 28, 41 and 46), we observed insertions of 3 to 9 small fragments (19-177 bp) derived from various

chromosomes (1,2,3,4,5,6,7,8,11,12,14,15,16,17 and 22) (Fig.2 and 3, supplemental data 1 and 3), resulting in 35 small inserted fragments. Taken these small insertions into account, this rearrangement resulted in 85 junctions. Twenty-three fragments of chromosome 14 were in an inverted orientation, as well as 18/35 small inserted fragments. We observed 2 to 7 bp microhomology (≥ 2bp) in 25/85 junctions. There were twenty-one deletions on chromosome 14 (from 723 bp to 1565077 bp) concordant with microarray analysis results (Fig.2). Besides these deletions, the rearrangement disrupted 10 OMIM genes (*FLRT2*, *EML5*, *FOXN3*, *RPS6KA5*, *CCDC88C*, *UNC79*, *SERPINA3*, *CLMN*, *GSKIP*, *YY1*).

Discussion

This case highlights the increasing complexity in genetic analysis and the fact that the different steps complement each other. Although karyotype is not considered any more as the first line laboratory examination in children presenting with developmental defects and/or intellectual disability, many laboratories continue to perform standard chromosome analysis, in parallel with molecular techniques like SNP-Array or next-generation sequencing, since it allows the rapid diagnosis of most balanced chromosomal rearrangements. When associated with an abnormal phenotype, these latter are of importance in the identification of new genes responsible for these pathologies. This strategy, from karyotype to NGS, is still justified since whole genome sequencing is not yet widely available in current diagnosis.

In our patient, karyotyping revealed that one chromosome 14 showed an unusual banding pattern on the long arm, thus leading to further investigations by SNP array. It allowed to detect 13 deletions and to confirm the *de novo* occurrence of the event on the paternal chromosome. However, deleted and interrupted genes, as identified by

this technique, didn't explain fully the phenotype of the patient suggesting that the situation was more complex than expected and needing more sensitive methods like Next Generation Sequencing (NGS).

Therefore, whole genome sequencing (WGS) was conducted and breakpoint cloning identified 50 breakpoints and insertions of fragments involving 15 different chromosomes, thus allowing a better characterization of this rearrangement and new relationships between genes and the patient's phenotype.

Usually, chromoanagenesis in the context of congenital disorders involves one or few chromosomes [5]. In our case, NGS revealed dramatically complex chromosomal events since it involved 15 different chromosomes. Regarding to the chromotripsis mechanism, firstly by analyzing ten constitutional CCRs, Kloosterman et al. (2012) concluded that chromosome shattering by multiple DSBs and non-homologous repair may be a common mechanism underlying chromothripsis rearrangements [13]. More recently, Zhang et al. [14] demonstrated that the mechanism for chromothripsis can involve the fragmentation and subsequent reassembly of a single chromatid from a micronucleus, providing an explanation for the restriction of chromothriptic rearrangements to a single chromosome.

We showed that the rearrangement had occurred *de novo* on the paternal chromosome 14. This is in agreement with previous reports that demonstrated the occurrence of this kind of events in the germline, as well as a paternal bias for CNV or CCR formation [17,18]. The deletions, insertions and inversion pattern identified in this case approached the pattern reported by Nazaryan-Petersen et al, and reinforced the probability of a chromotripsis mechanism.[19]

Owing to data obtained from both SNP-array and WGS in our patient, we were able to establish valuable genotype-phenotype correlations. In the literature, few patients with

pure terminal deletions of 14q, with or without ring chromosome formation, and characterized by molecular cytogenetic methods have been reported [20,21,8]. A recurrent 1.11 Mb microdeletion of 14q32.2 including the *DLK1/GTL2* imprinted gene cluster, mediated by expanded TGG repeats, has also been described in two unrelated patients presenting with clinical features compatible with UPD (14)mat [22]. In our report, the imprinted region on 14q was not involved, as determined by SNP-array and this finding was confirmed by direct analysis of the methylation profile of the *DLK1/GTL2* region (data not shown). Typical clinical features of the 14q terminal deletion syndrome include developmental delay, hypotonia, growth retardation, microcephaly, a characteristic facial appearance and a variety of ocular anomalies, including retinal pigmentary changes, microphthalmia and coloboma [8]. Similar phenotypic features were present in our patient, including chorioretinal coloboma. The structural eye defects, microphthalmia, anophthalmia and coloboma (MAC) have a large genetic component with several loci of genes located in the proximal and central parts of the 14q arm [8]. Review of the literature suggests that an additional locus for coloboma may map to the terminal region of 14q32.31 [8 21]. In our case, the deleted regions, although in the vicinity of the MAC spectrum locus, do not overlap with it but could have position effects altering the expression of intact genes near the breakpoints. Alternatively, as suggested by Salter et al. (2016), the possibility of an underlying multigenic mechanism could to be considered. Indeed, our patient was also presenting with a hypoplastic corpus callosum. Agenesis or dysgenesis of the corpus callosum is a heterogeneous condition, for which several different genetic causes are known. Interestingly, in the literature, an abnormal corpus callosum had previously been reported in four patients with a 14q32 deletion, suggesting that a gene involved in corpus callosum development may map to this region [23]. A chromoanagenesis on chr 14 has been

reported in a patient with developmental delay, characterized by the deletion of 2.7 Mb in 14q32.33 and the insertion of 4q32.3 into the long arm of chromosome 14.[24] Developmental delay fit with our case, but no other phenotypical features were fitting between the two cases.

In our patient, the deleted regions contain genes like *EML1*, encoding for Echinoderm microtubule-associated protein-like 1 which is expressed in eye and associated to the photoreceptor [25] or *CYP46A1*, encoding for cytochrom oxydase 46A1 which is involved in brain cholesterol metabolism [26]. Loss of *CYP46A1*, which may play an important role in brain tissue, may be responsible for the neurologicals disorders observed in patients with 14q deletion [27]. In the inserted fragments, no argument (content, localization or orientation) was found to explain the patient's phenotype. In addition, breakpoint analysis by genome sequencing revealed the interruption of 10 genes: *EML5*, *FOXN3*, *RPS6KA5*, c14orf159, *CCDC88C*, *UNC79*, *SERPINA3, CLMN, GSKIP, YY1*. This latter encodes for a zinc-finger transcription factor involved normal development and malignancy. Deletions of *YY1* have been associated with cognitive impairments, behavioral alterations, intrauterine growth restrictions, feeding problems, and various congenital malformations [28]. These features could correspond to the phenotype in our patient but with less severe issues. However, although eyes abnormalities (strabism and hypermetropia) have been reported in 3 patients in the cohort of Gabriele-de Vriess syndrome, coloboma has not been associated with this syndrome.

In conclusion, this report highlights the complementarity of different genomic investigation techniques leading to a better comprehension of the mechanism in CCR events, therefore leading to a better genetic counselling to the families.

Acknowledgments

We thank the technical team of the cytogenetic laboratory for their excellent assistance.

Legend

FIGURE 1

G-Banding, FISH and SNP array analyses.

A: Representative pair of G-banded chromosome 14. The distal region of the q arm showed an abnormal banding pattern on one chromosome (arrow). **B**: FISH using the Whole Chromosome Painting Probe 14 (wcp14 spectrum green, Metasystem). **C**: FISH using subtelomere 14q probe (spectrum orange, hg19, chr14:107,159,193-107,268,415) and LSI TCR 14q11.2 probe (spectrum aqua) (Vysis), showing signals on both 14 chromosomes. **D**: FISH using BAC RP11-300J18 (14q31.3) (spectrum red, hg19, chromosome14:88,484,949-88,502,663) spanning one deleted region (308 K) and 14qtel probe (spectrum green, hg19, chromosome 14:107,159,193-107,268,415, Vysis) do not show red signal on the der(14q) chromosome (arrow). **E**: SNP-array profile of the terminal region of the long arm of chromosome 14 showing 13 deletions clustered at 14q31.1-q32.2. B allele frequency and logR ratio are shown in the upper panel. Orange bands indicate deleted regions. **F**: Genome studio representation of the rearranged region between 14q31.1 and 14q32.2 bands (chr14: 83,088,298-100,452,660), and the OMIM deleted genes.

FIGURE 2

Circos plot issue from the WGS data, showing clustering of the breakpoints on chromosome 14 and the involvement of 15 other chromosomes.

FIGURE 3: Example of breakpoint junction number 41 structure. On the left, schematic representation of the recombined region, with the different chromosomes' regions represented by different colors. On the right, the details of the junction, the underlined nucleotides correspond to homology region.

Bibliography:

[1] Zhang F, Carvalho CM, Lupski JR. Complex human chromosomal and genomic rearrangements. *Trends Genet* 2009; **25**: 298-307.
[2] Kloosterman WP, Guryev V, van Roosmalen M, Duran KJ, de Bruijn E, Bakker SC, et al. Chromothripsis as a mechanism driving complex de novo structural rearrangements in the germline. *Hum Mol Genet* 2011; **20**: 1916-1924.
[3] Liu P, Erez A, Nagamani SC, Dhar SU, Kołodziejska KE, Dharmadhikari AV, et al. Chromosome catastrophes involve replication mechanisms generating complex genomic rearrangements. *Cell* 2011; **146**: 889-903.
[4] Stephens PJ, Greenman CD, Fu B, Yang F, Bignell GR, Mudie LJ, et al. Massive genomic rearrangement acquired in a single catastrophic event during cancer development. *Cell* 2011; **144**: 27-40.
[5] Masset H, Hestand MS, Van Esch H, Kleinfinger P, Plaisancié J, Afenjar A, et al. A Distinct Class of Chromoanagenesis Events Characterized by Focal Copy Number Gains. *Hum Mutat* 2016; **37**: 661-668.
[6] Pellestor F, Anahory T, Lefort G, Puechberty J, Liehr T, Hédon B, et al. Complex chromosomal rearrangements: origin and meiotic behavior. *Hum Reprod Update* 2011; **17**: 476-494.
[7] de Pagter MS, van Roosmalen MJ, Baas AF, Renkens I, Duran KJ, van Binsbergen E, et al. Chromothripsis in healthy individuals affects multiple protein-coding genes and can result in severe congenital abnormalities in offspring. *Am J Hum Genet* 2015; **96**: 651-656.
[8] Salter CG, Baralle D, Collinson MN, Self JE. Expanding the ocular phenotype of 14q terminal deletions: A novel presentation of microphthalmia and coloboma in ring 14 syndrome with associated 14q32.31 deletion and review of the literature. *Am J Med Genet A* 2016; **170A**: 1017-1022.
[9] H L. Aligning sequence reads,
clone sequences and assembly contigs with BWA-MEM.arXiv:1303.3997 [q-bio.GN]: arXiv:1303.3997 [q-bio.GN] 2013.
[10] Li H, Handsaker B, Wysoker A, Fennell T, Ruan J, Homer N, et al. The Sequence Alignment/Map format and SAMtools. *Bioinformatics* 2009; **25**: 2078-2079.
[11] Chen K, Wallis JW, McLellan MD, Larson DE, Kalicki JM, Pohl CS, et al. BreakDancer: an algorithm for high-resolution mapping of genomic structural variation. *Nat Methods* 2009; **6**: 677-681.
[12] Thorvaldsdóttir H, Robinson JT, Mesirov JP. Integrative Genomics Viewer (IGV): high-performance genomics data visualization and exploration. *Brief Bioinform* 2013; **14**: 178-192.
[13] Kloosterman WP, Tavakoli-Yaraki M, van Roosmalen MJ, van Binsbergen E, Renkens I, Duran K, et al. Constitutional chromothripsis rearrangements involve clustered double-stranded DNA breaks and nonhomologous repair mechanisms. *Cell Rep* 2012; **1**: 648-655.
[14] Zhang CZ, Spektor A, Cornils H, Francis JM, Jackson EK, Liu S, et al. Chromothripsis from DNA damage in micronuclei. *Nature* 2015; **522**: 179-184.
[15] Macera MJ, Sobrino A, Levy B, Jobanputra V, Aggarwal V, Mills A, et al. Prenatal diagnosis of chromothripsis, with nine breaks characterized by karyotyping, FISH, microarray and whole-genome sequencing. *Prenat Diagn* 2015; **35**: 299-301.
[16] Collins RL, Brand H, Redin CE, Hanscom C, Antolik C, Stone MR, et al. Defining the diverse spectrum of inversions, complex structural variation, and chromothripsis in the morbid human genome. *Genome Biol* 2017; **18**: 36.
[17] Hehir-Kwa JY, Rodríguez-Santiago B, Vissers LE, de Leeuw N, Pfundt R, Buitelaar JK, et al. De novo copy number variants associated with intellectual disability have a paternal origin and age bias. *J Med Genet* 2011; **48**: 776-778.

[18] Fukami M, Shima H, Suzuki E, Ogata T, Matsubara K, Kamimaki T. Catastrophic cellular events leading to complex chromosomal rearrangements in the germline. *Clin Genet* 2017; **91**: 653-660.
[19] Nazaryan-Petersen L, Eisfeldt J, Pettersson M, Lundin J, Nilsson D, Wincent J, et al. Replicative and non-replicative mechanisms in the formation of clustered CNVs are indicated by whole genome characterization. *PLoS Genet* 2018; **14**: e1007780.
[20] Zollino M, Ponzi E, Gobbi G, Neri G. The ring 14 syndrome. *Eur J Med Genet* 2012; **55**: 374-380.
[21] Engels H, Schüler HM, Zink AM, Wohlleber E, Brockschmidt A, Hoischen A, et al. A phenotype map for 14q32.3 terminal deletions. *Am J Med Genet A* 2012; **158A**: 695-706.
[22] Béna F, Gimelli S, Migliavacca E, Brun-Druc N, Buiting K, Antonarakis SE, et al. A recurrent 14q32.2 microdeletion mediated by expanded TGG repeats. *Hum Mol Genet* 2010; **19**: 1967-1973.
[23] Schneider A, Benzacken B, Guichet A, Verloes A, Bonneau D, Collot N, et al. Molecular cytogenetic characterization of terminal 14q32 deletions in two children with an abnormal phenotype and corpus callosum hypoplasia. *Eur J Hum Genet* 2008; **16**: 680-687.
[24] Kato T, Ouchi Y, Inagaki H, Makita Y, Mizuno S, Kajita M, et al. Genomic Characterization of Chromosomal Insertions: Insights into the Mechanisms Underlying Chromothripsis. *Cytogenet Genome Res* 2017; **153**: 1-9.
[25] Korenbrot JI, Mehta M, Tserentsoodol N, Postlethwait JH, Rebrik TI. EML1 (CNG-modulin) controls light sensitivity in darkness and under continuous illumination in zebrafish retinal cone photoreceptors. *J Neurosci* 2013; **33**: 17763-17776.
[26] Lund EG, Xie C, Kotti T, Turley SD, Dietschy JM, Russell DW. Knockout of the cholesterol 24-hydroxylase gene in mice reveals a brain-specific mechanism of cholesterol turnover. *J Biol Chem* 2003; **278**: 22980-22988.
[27] Repnikova EA, Astbury C, Reshmi SC, Ramsey SN, Atkin JF, Thrush DL, et al. Microarray comparative genomic hybridization and cytogenetic characterization of tissue-specific mosaicism in three patients. *Am J Med Genet A* 2012; **158A**: 1924-1933.
[28] Gabriele M, Vulto-van Silfhout AT, Germain PL, Vitriolo A, Kumar R, Douglas E, et al. YY1 Haploinsufficiency Causes an Intellectual Disability Syndrome Featuring Transcriptional and Chromatin Dysfunction. *Am J Hum Genet* 2017; **100**: 907-925.

Figure 1

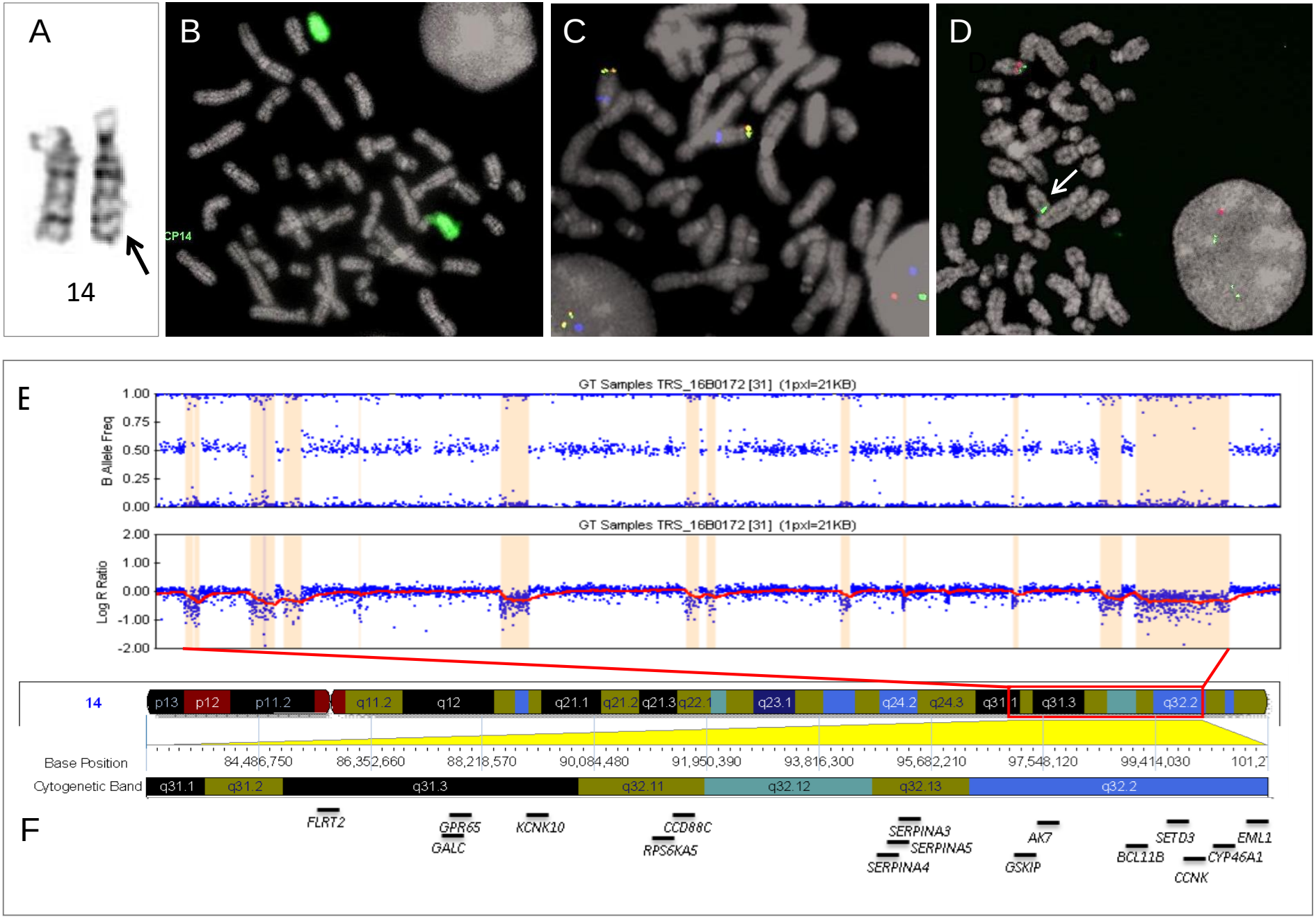
A
14
B
CP14
C
D
E
GT Samples TRS_16B0172 [31] (1pxl=21KB)
B Allele Freq
1.00
0.75
0.50
0.25
0.00
GT Samples TRS_16B0172 [31] (1pxl=21KB)
Log R Ratio
2.00
1.00
0.00
-1.00
-2.00
14
p13 p12 p11.2 q11.2 q12 q21.1 q21.2 q21.3 q22.1 q23.1 q24.2 q24.3 q31.1 q31.3 q32.2
Base Position
84,486,750 86,352,660 88,218,570 90,084,480 91,950,390 93,816,300 95,682,210 97,548,120 99,414,030 101,2
Cytogenetic Band
q31.1 q31.2 q31.3 q32.11 q32.12 q32.13 q32.2
F
FLRT2
GPR65
GALC
KCNK10
CCD88C
RPS6KA5
SERPINA3
SERPINA5
SERPINA4
AK7
GSKIP
SETD3
BCL11B
CCNK
CYP46A1
EML1

Figure 2

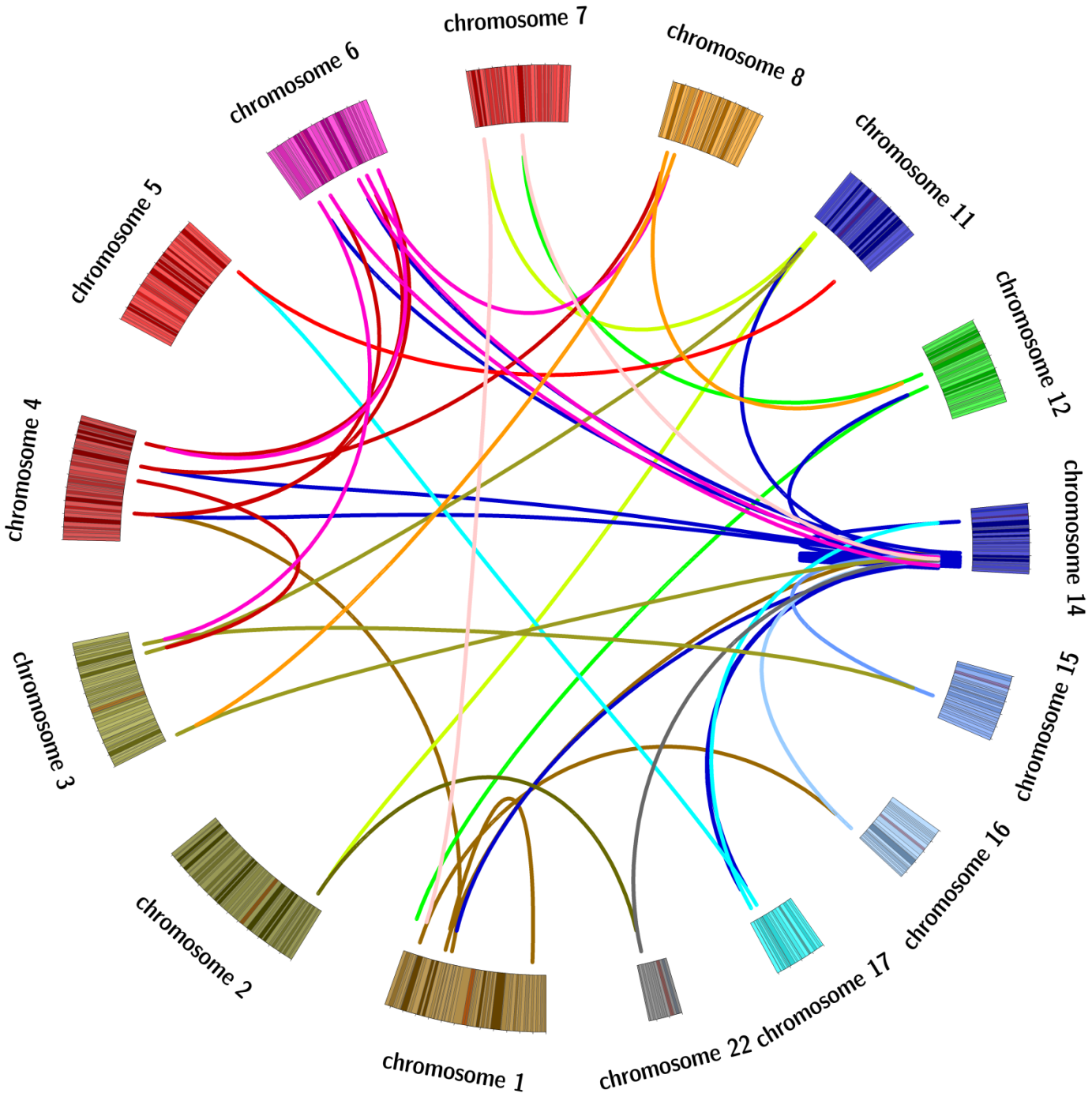
chromosome 7
chromosome 8
chromosome 6
chromosome 11
chromosome 5
chromosome 12
chromosome 4
chromosome 14
chromosome 3
chromosome 15
chromosome 16
chromosome 2
chromosome 17
chromosome 22
chromosome 1

Figure 3

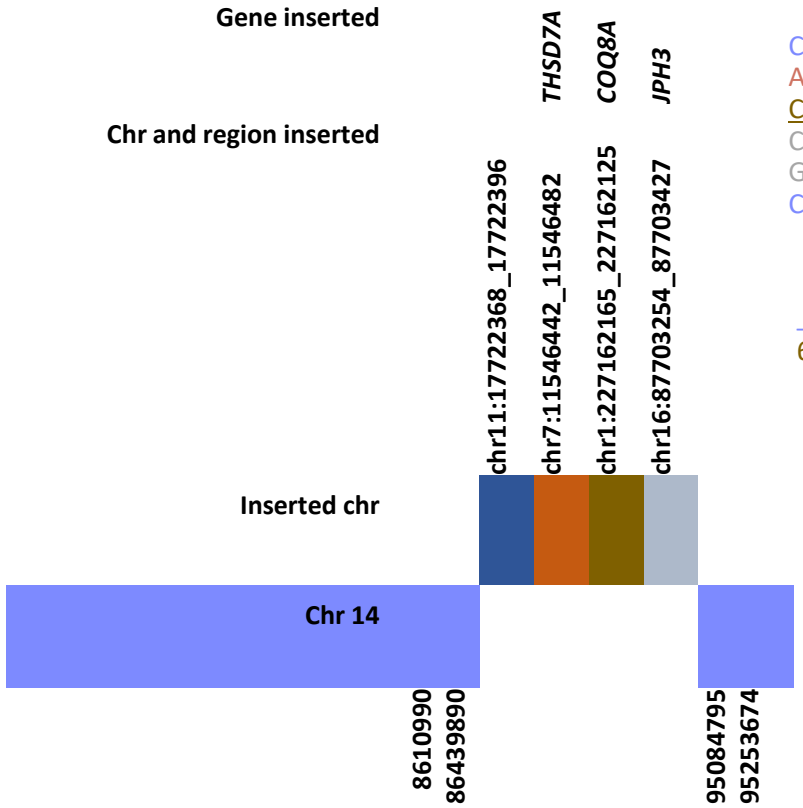

CTTCTCAAGGAGTACCTTTGCGGTCTTTATAAGTTCCTGTTATGGGCCAGACAACTTCTATCTTCCT
AGAGAGTCTTTGCATGACCCACCTGTCCTCACACCTCTCCCTGCTCAGATCCACATTCTAAGAGCGC
CTGGCGTGTGGGGTGGAGGCCGGGACAGTGTGAGGGCCGCCTGGTCAGAGCGGGAGGCAGGA
CCCCGTAGGGAGATGAAAGCCAAGCTGGACCCAGGCAGAAAAAGAGGAACGAAGGACAGGAA
GTCCAAGAGCAGTCACTGCTGACGTGAGTGCGGCCTGCAGGCAGCCAGTGTACTGAATCCAGGG
CAAATCTTAGCT

_chr14:86439890::chr11:17722368_17722396::chr7:11546442_11546482::chr1:227162165_227162125::chr16:87703254_87703427::chr14:95084795_